Functionalized Cochlear Implant electrode for intracochlear histamine detection via Molecular Imprinted Polymer (MIP) coating

Tristan Putzeys, Gideon Wackers, Oliver Jamieson, Marloes Peeters, Theodor Doll, Patrick Wagner, Michael Wübbenhorst, Nicolas Verhaert*

Tristan Putzeys, Nicolas Verhaert
KU Leuven, Research Group Experimental Oto-rhino-laryngology, O&N II, Herestraat 49, B-3000 Leuven, Belgium
E-mail: Tristan.putzeys@kuleuven.be

Tristan Putzeys, Gideon Wackers, Patrick Wagner, Michael Wübbenhorst
KU Leuven, Laboratory for Soft Matter and Biophysics, Celestijnenlaan 200 D, B-3001 Leuven, Belgium

Oliver Jamieson, Marloes Peeters
Newcastle University, School of Engineering, Newcastle NE1 7RU, United Kingdom

Theodor Doll
Hannover Medical School, Institute of AudioNeuroTechnology VIANNA, Stadtfelddamm 34, D-30625 Hannover, Germany

Nicolas Verhaert
University Hospitals Leuven, Department of Otorhinolaryngology, Head and Neck Surgery, B–3000 Leuven, Belgium

Keywords: biosensors, electrical impedance, non-faradaic, inflammation, equivalent-electronic-circuit

0. Abstract

By coating the electrodes of a Cochlear Implant (CI) electrode array with a powdered form of molecular imprinted polymer (MIP), we demonstrate a straightforward process to functionalize existing electrodes to selectively detect histamine. Detection is based on non-Faradaic impedance spectroscopy, omitting the need for a reference electrode or redox mediators, and

fitting to a 5-element equivalent electronic circuit. Proof-of-concept measurements on three functionalized cochlear implants in three human cadaveric cochleae indicated a level of detection of 200 nM of histamine in albumin-based artificial perilymph following a sigmoid dose-response trend up to 10 mM. This sensitivity enables quantized and localized analysis of histamine-mediated inflammation immediately following the CI operation. The selectivity and adaptability of MIPs opens possibilities to detect a wide spectrum of inflammation markers inside the human cochlea and could be used for fast mid- or postoperative intervention to improve the medical implant's outcome.

1. Introduction

A Cochlear Implant (CI) is a neuroprosthetic device that partially restores hearing by direct stimulation of the auditory nerve fibers, bypassing the conventional hearing pathway.[1] It is a successful option for individuals suffering from severe hearing loss who cannot be helped by sound pressure amplifying hearing aids. An electrode array is surgically inserted inside one of the cochlear ducts, the scala tympani, and contains platinum electrodes that allow electrical pulses to be applied inside the cochlea and trigger neurons to simulate hearing. As the CI surgeon relies mostly on tactile feedback, the insertion itself is not without risk and soft tissue can be damaged, this is known as insertion trauma and is a well-studied topic in implant surgeries.[2]–[5] Even when insertion trauma does not occur, the cochlea can still exert a foreign body reaction to the implant, encapsulating it in tissue and resulting in chronic inflammation.[6] While advances have been made in preventing trauma associated with cochlear implant insertion, such as softer electrode design, functional monitoring of residual hearing and radiographic-based planning, little is known on the actual correlation between insertion trauma and the electrophysiological- and biochemical response to inflammation.[7]–[9]

Inflammation is typically a beneficial reaction intended to protect against infections and tissue injury[10] and can help establish an immunological memory for a better future response against a particular source of infection.[11], [12] The cochlea used to be classified as an immune-privileged system where antigens do not invoke an inflammatory immune response as it is isolated by a tight Blood-Labyrinth Barrier.[13] This has largely been dismissed by both the findings of resident macrophages in the lateral wall and the scala tympani[14], and also by the correlation between BLB permeability and inflammatory cytokines in the spiral ligament and stria vascularis.[14]–[16] Studies have found that inflammation within the cochlea can be a response to not only pathogens[17], but also to ototoxic drugs[18], noise trauma[19], cochlear surgery, and the presence of a cochlear implant.[20]

Histamine is often involved as an inflammatory mediator as a vasoactive amine that increases vasodilation and vascular permeability, allowing white blood cells and proteins to reach the site of injury or infection.[21] It consists of an imidazole ring attached to an ethylamine chain, under physiological conditions the amino group (-NH2) is protonated. Histamine is generated and stored in granules in mast cells and in basophiles (white blood cells) by decarboxylation of the amino acid histidine.[22] After release, such as after degranulation of the cell, histamine is rapidly inactivated by degradative enzymes. In plasma, histamine has a recorded life-time in the order of 60 seconds.[23], [24] An increase can be indicative for the occurrence of an acute non-immune inflammation,[25] but the limited half-life makes it difficult to measure the amine concentration using high-resolution gas chromatography or optical ELISA (enzyme-linked immunosorbent assay).

A histamine-sensitive coating applied to a cochlear implant electrode array would allow us to measure the intracochlear histamine concentration. It would also shed light on the role of histamine in the cochlea as histamine receptors and histamine-immunoreactive nerve fibers have been found in the cochlea of rodents,[26], [27] yet little is known on the pathways involved.[21] The histamine-sensitive coating can be made of enzymes or antibodies to recognize histamine molecules, or a synthetic organic polymer coating with a high affinity for the analyte. The former suffers from poor long-term stability in biological active environments, rendering them less suitable for implantable devices.[28] Synthetic coatings circumvent degradation by biological processes due to their inherent resilience to pH-, oxidative stress- or biodegradation, as demonstrated in histamine detection in acidic bowel fluids from the gastrointestinal tract.[29] In this research we have opted for synthetic Molecularly Imprinted Polymers (MIPs) as coating with a receptor functionality.

MIPs are polymers that have been imprinted with a target molecule. This imprinting is usually done by polymerizing functional monomers in the presence of template molecules, which are later extracted using organic solvents, acids, or bases, resulting in complementary cavities. These cavities have a high affinity for the template molecule due to similarities in size and shape and the embedding of functional groups in the walls of the cavities.[30] When the empty MIP coating encounters the target molecule it displaces the solvent, an aqueous liquid in biological systems, that was originally inside the polymer cavity. This displacement changes the (thermal or electrical) resistance of the coating. The change in impedance is directly related to the concentration of the target molecules, typically according to a sigmoid dose-response. [29] Measuring the change in electrical impedance is advantageous for CI electrodes as they require minimal adaptation. An electrical driving and, albeit simplified, impedance analysis circuit is

already present in the external hardware of the hearing aid. The extremely small volume of the cochlear canal, in the order of 80 µL,[31] makes thermal sensing, such as the hotwire technique,[32] an unsuitable option, as the temperature increase is difficult to contain and could induce thermal lysis.

Here, we demonstrate the feasibility of detecting histamine inside the scala tympani in three different human cochleae via MIP-functionalized cochlear implants, using non-Faradaic, electrical impedance spectroscopy, without the need for a reference electrode or redox mediators. The aim is to develop a straightforward to integrate chemical sensor on cochlear implants to study inflammatory reactions inside the cochlea.

2. Methods

2.1. MIP Synthesis

MIP receptors were synthesized by photopolymerization of acrylic acid in the presence of histamine, from histamine chloride, utilizing ethylene glycol dimethacrylate as the cross-linker monomer and dimethyl sulfoxide as the porogen, i.e. to facilitate diffusion of the target molecules to the actual binding sites by increasing the porosity of the resulting polymer. All chemicals were purchased from Acros (Loughborough, United Kingdom) with a purity better than 99%. A detailed description of the histamine-selective MIP synthesis protocol and associated cross-selectivity tests (against betahistine and histidine) can be found by Wackers et al. and Peeters et al. [29], [33] Following polymerization, the polymer was ground to a fine powder and passed through a sieve, after which the template molecules were removed using organic solvents in a Soxhlet extractor. The powder was then vacuum dried and stored under ambient conditions.

2.2. CI functionalization

The CIs used were 3 existing 8-electrode HL08 flexible animal electrode arrays from Cochlear (Cochlear Ltd. Australia, Sydney) and one custom-made 8-electrode implant manufactured by the Hannover Medical School (MHH, Hannover, Germany). To attach the dried MIP powder to the electrodes of a CI, a viscous adhesive layer of polystyrene (918 kDa, 50 mg/mL toluene) (Polymer Source Inc. Montreal, Canada) was first applied to the platinum electrodes. The “wet” CI was then gently rolled into the MIP powder to ensure full electrode coverage. Conditioning at a temperature of 130 °C for 120 minutes evaporated the toluene solvent. Since not all the powder particles were bound with the polystyrene, the electrode array was washed with distilled water to remove these particles, preventing them from interfering with later measurements. Functionality of the CI was tested in 1xPBS solution before and after MIP coating. A

photograph comparing the three MIP coated CIs is included in Figure 1. All have the same base polystyrene coating but differ in the amount of MIP particles attached to them due to differences in MIP particle size. The labels associated with each electrode corresponds to the cochlea it was implanted in. Both fresh Temporal bone (TB), and Fresh Frozen Temporal bone (FFTB) were used. Fresh signifies the specimen was provided with no freezing storage step between harvest and measurement, while fresh frozen means the cochlea experienced at least one freezing and thawing cycle. One original HL08 electrode array was used to measure the native and artificial perilymph in a non-frozen temporal bone for validation of the electrochemical properties of the artificial perilymph. Coating increased the diameter of the CI electrode array from 640 to 940 µm for TB1, from 640 to 700 µm for FFTB2, and from 500 to 900 µm for FFTB3. The scala tympani of the cochlea has a minor diameter of approximately 1mm or 1000 µm in the first 180° turn. [34]

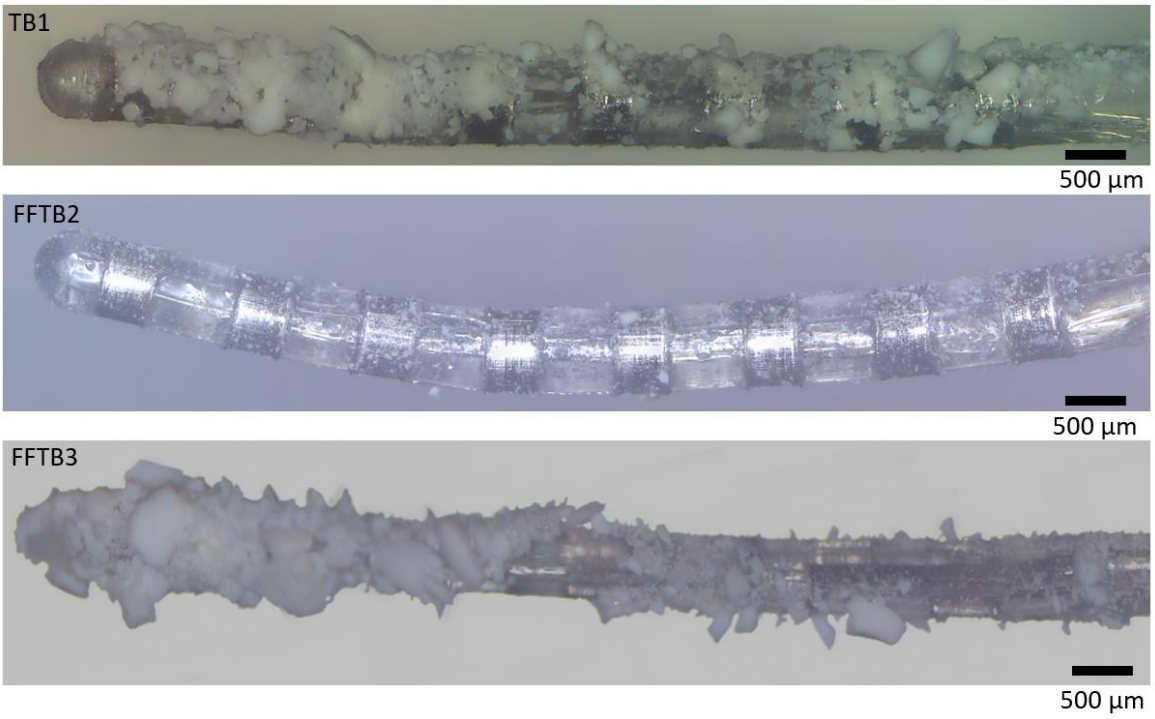

Figure 1. Three MIP-coated CIs labeled TB1, FFTB2 and FFTB3. FFTB2 has the lightest coating, TB1 has slightly more MIP powder attached and FFTB3 has a dense coating of MIP particles, as proof-of-concept.

2.3. Sample preparation

One fresh (TB1) and two fresh-frozen human temporal bones (FFTB2 and FFTB3), provided by the Vesalius Institute (KU Leuven, Belgium) were used during the experiments. The experimental protocols were approved by the Medical Ethics Committee of the University Hospitals of Leuven, approval Number S65502. No biographical donor data is known.

Temporal bones containing the cochlea were harvested and used in accordance with the Helsinki declaration from individuals who gave informed consent.

Bone and soft tissue were removed from the temporal bone (mastoidectomy and posterior tympanotomy) until the cochlea was exposed and both the round window membrane, the stapes footplate and the apex of the cochlea was accessible. The functionalized CI was inserted via the round window membrane (RWM) into the scala tympani (ST), similar to standard minimally invasive CI insertion techniques,[35] photograph in Figure 2. Samples that were stored fresh frozen were no longer electrochemically or impedimetrically representative,[36] the contents of the cochleae were therefore flushed with artificial perilymph via either the stapes footplate or an artificial opening in the apex (cochleostomy).

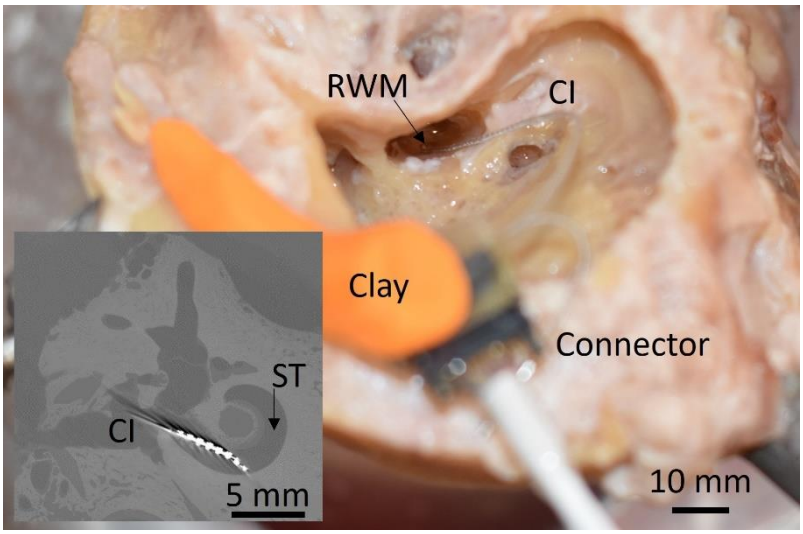

Figure 2. Photograph of a CI inserted via the round window membrane (RWM) in a fresh temporal bone. Orange clay is used to keep the CI and interface connector in place during handling. (Inset) Micro CT scan of temporal bone with HL08 CI inserted via the RWM into the Scala Tympani (ST). Scalebars for reference. Larger figure available in supplementary information.

2.4. Artificial Perilymph

Artificial perilymph is an albumin-based solution that electrochemically matches human perilymph, using the composition proposed by Palmer et al.[37] Its primary use is to replace the original perilymph which has undergone a freezing and thawing cycle, drastically changing its impedimetric response and can be produced in large quantities which allows for easier handling. The exact composition is known, making it an ideal reference liquid to spike with defined concentrations of histamine. It also does not contain living cells and is less prone to time-dependent effects.[36]

2.5. Data acquisition and analysis

Impedance spectra were acquired using a Novocontrol Alpha Analyzer with dielectric interface. An AC signal was applied with a peak-to-peak amplitude of 65 mV, to avoid unwanted cell depolarization[38] in non-Faradaic circumstances, i.e. without redox mediators in the perilymph. The use of these mediators would not be allowed in future clinical trials or patient studies and are therefore also not used in this study. A spectrum is recorded from 100 Hz to 1 MHz (7.5 measurements per decade). Selection of an electrode pair for impedance spectroscopy is made possible by an external Arduino-based multiplexer using shielded relays.

After insertion of a CI electrode array, the contents of the cochlea is flushed twice by 1 mL of artificial perilymph via syringe injection into either the stapes footplate or opening in the apex of the cochlea similar to previously described techniques.[39] This exceeds by far the volume of initial perilymph of 0.15 mL[40] and ensures a complete replacement of the intracochlear fluid with a known substance. Changing the histamine concentration involves flushing the cochlea twice with a 1 mL histamine-spiked artificial perilymph solution, ranging from 1 nM to 10 mM. Histamine concentrations above 100 µM are not expected under physiological conditions but are included to showcase upper detection limits of the sensor. After each injection, the fluid is allowed to settle for a few minutes, enabling air bubbles to vacate and the fluid-soft tissue system to reach a thermal and chemical equilibrium. All measurements occurred at room temperature of 18°C.

Data are processed and analyzed via Matlab (r2022b, Mathworks). The electrical impedance of the MIP coating is determined by fitting an appropriate equivalent electronic circuit (EEC) to the acquired spectrum, as described by Wackers et al[29]. and Stilman et al[41].

3. Results

One original and three functionalized CIs were inserted in a fresh-frozen temporal bone. The native perilymph was replaced by histamine-spiked artificial perilymph of various concentration, to simulate one particular aspect of acute inflammation. The impedimetric response of the artificial perilymph is compared to that of native perilymph from a fresh, non-frozen sample. The position of the CI is verified via microscope and the impedimetric response is fitted against an EEC to determine the resistance of the sensor coating and obtain the dose-response curve. Following the findings of Wackers et al.[29], histamine measurements were measured between the two top MIP coated electrodes as this is more accurate than measuring between a MIP-functionalized electrode and a metallic, non-coated electrode.

3.1. Electrical properties of Artificial perilymph

A non-functionalized CI (HL08, Cochlear) was inserted in a fresh temporal bone and the impedance spectrum of the native perilymph was recorded with the electrodes of this CI. Afterwards, the contents of the cochlea were flushed via the oval window with artificial perilymph and the spectra are compared for impedimetric mimetics. A comparison of both capacitance (directly measured by the Novoconrol Alpha-analyzer) and impedance is given in Figure 3. The artificial perilymph is based on human serum albumin, which tends to absorb to surfaces and increases the low frequency capacitance, slightly lowering the overall impedance. This effect is only visible below 100 Hz, above this frequency the two liquids are impedimetrically equivalent.

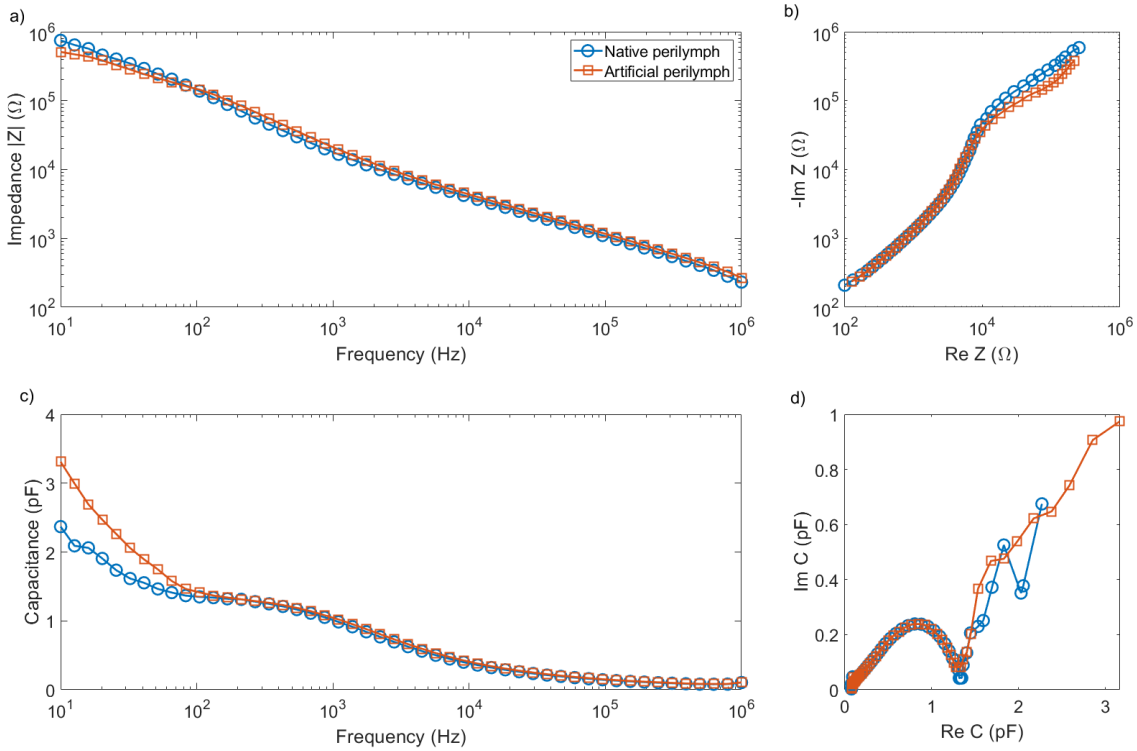

Figure 3. a) Impedance of both native and artificial perilymph as measured by a non-functionalized cochlear implant electrode array inserted in the scala tympani of a human cochlea. a) is absolute value of the impedance while b) is the Nyquist plot of the imaginary part of the impedance versus the real part of the impedance. c) Capacitive spectrum of both native and artificial perilymph displayed as both the absolute value in function of frequency and d) as a Nyquist plot. Below 100 Hz the artificial perilymph has a lower impedance and a higher capacitance due to surface absorption of human serum albumin.

3.2. Impedance spectra

In all temporal bones, the cochlear perilymph was replaced by artificial perilymph with exponentially increasing concentration of histamine chloride salt, ranging from 1nM to 10 mM.

For each concentration increase the intracochlear impedance of the perilymph was recorded in the range of 100 Hz to 100 kHz with an AC signal of 65 mV peak-to-peak (or 46 mVrms). Example results of impedance amplitude and phase measured at 5 nM and 10 µM histamine concentration are represented graphically in Figure 4. Impedance spectra for all three CI electrode arrays over the full histamine concentration range are included in the supplementary information. Variance in both PolyStyrene (PS) and MIP powder coating thickness result in variation in both initial impedance and change in impedance between samples.

3.3. Equivalent Electronic Circuit (EEC) fitting and dose response behavior

Each of the recorded impedance spectra is fitted to an equivalent electronic circuit: The sensor coating is modelled as a parallel circuit of an ohmic resistance and a capacitor (R1 and C1 in Figure 4), in series with a Warburg impedance (Aw) representing the coating-liquid interface, and an ohmic resistance representing the sum of cable resistance and liquid conductivity (Rs). Building further on previous studies[29], [41] in intestinal fluids or PBS, the sensor/liquid interface is modelled as also having a capacitive double layer (Cdl), rather than only a Warburg impedance (Aw). This increases the number of fitting parameters from 4 to 5. Fitting occurs to both the amplitude and phase of the impedance spectrum. An example is given in Figure 4, where both the amplitude and phase of the impedance and the associated best EEC fit is given for two different concentration levels of histamine, 5 nM vs. 10 µM in TB1. The spectrum of perilymph spiked to 10 µM introduces a noticeably larger impedance below 10 kHz when measured with a MIP-functionalized CI electrode, also the region with the lowest phase lag shifts to higher frequencies by approximately one decade, from 10 to 100 kHz. The R^2 value of the fit is 0.994 and 0.966 respectively for a concentration of 5nM and 10 µM histamine chloride. Calculation of the dose response behavior will be based on the R1 value of the chemical sensor coating in the 5-element model.

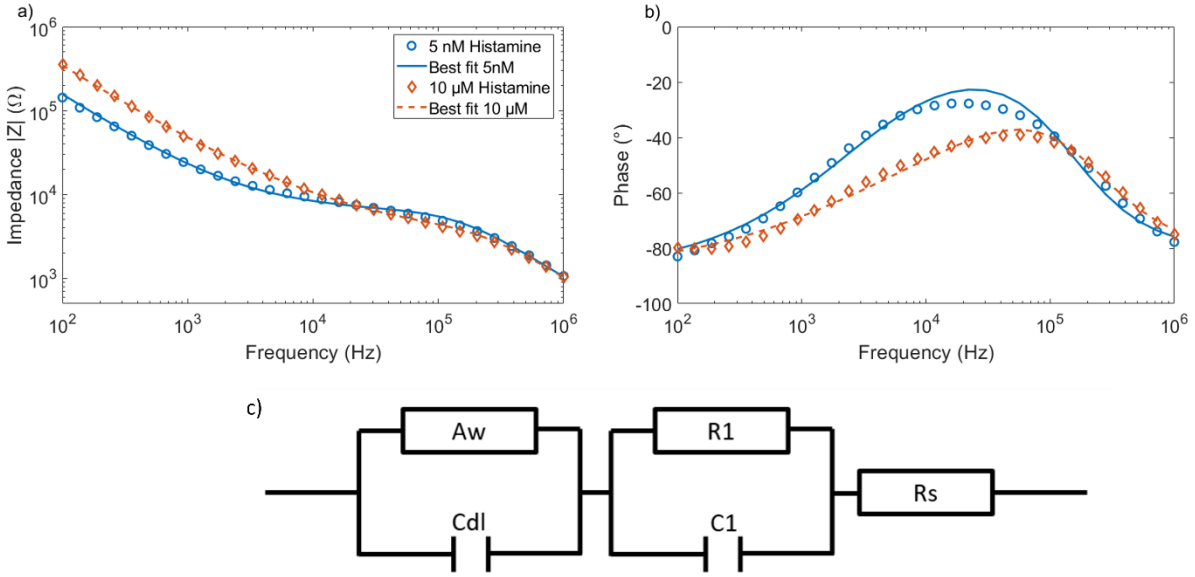

Figure 4. a) and b) Amplitude and phase of the impedance spectrum of perilymph measured by a functionalized CI electrode in a 5 nM and a 10 µM histamine environment. Markers indicate individual data points and solid lines represent optimal fitting to the EEC in (c). Major changes in the amplitude are visible at the low frequency impedance, while in the phase the region with the smallest phase difference shifts to higher frequency. C) A 5 element EEC is used.

Fitting to different components allows for determining the ohmic resistance of the sensor coating (R1) and greatly reduces the influence of the changes in perilymph properties (Aw, Cdl and Rs) due to increasing histamine concentration. The change of sensor coating resistance in function of the histamine concentration in the artificial perilymph is given in Figure 5 for TB1, FFTB2 and FFTB3. Single data points are the ohmic resistance (R1) of the MIP layer as obtained by fitting the impedance spectra to the 5 element EEC model (Figure 4.c), the error bars correspond to the 95% margin of error as obtained by the fitting of that parameter to the model. The dashed line corresponds, in color, to the best fit obtained based on a sigmoid dose response function (Eq. 1), a common biological response function, of the resistance R1(c) in function of histamine concentration (c). The impedance response function is characterized by an initial value R1(c=0) when the target (Histamine) is absent. When fully saturated, the impedance will have increased with an amplitude A to a value of R1(c=0) + A. The function is most sensitive to change when the response is halfway between R1(c=0) and R1(c=0) + A, when the concentration c of the target is equal to ED50, the Effective Dose 50% concentration. S determines the slope of the curve; a higher value means a steeper curve and a higher sensitivity. All parameters must be real, positive numbers.

$$R(c) = R(c=0) + \frac{A}{1 + \left(\frac{ED_{50}}{c}\right)^{S}} \quad (1)$$

The left panel of Figure 5 displays the absolute value of the resistance of the MIP layer, while the right panel presents the same data normalized to the resistance when no histamine has been added to the artificial perilymph. For the spectra obtained, the best sigmoid dose response fit is given in Table 1. The plus-minus sign indicates the standard deviation on the obtained fitting result. Normalized R2 values are presented in the second to last column. The right-hand column contains the level of detection (LOD), which is the lowest concentration of histamine where the response equals three times the standard deviation of the baseline.

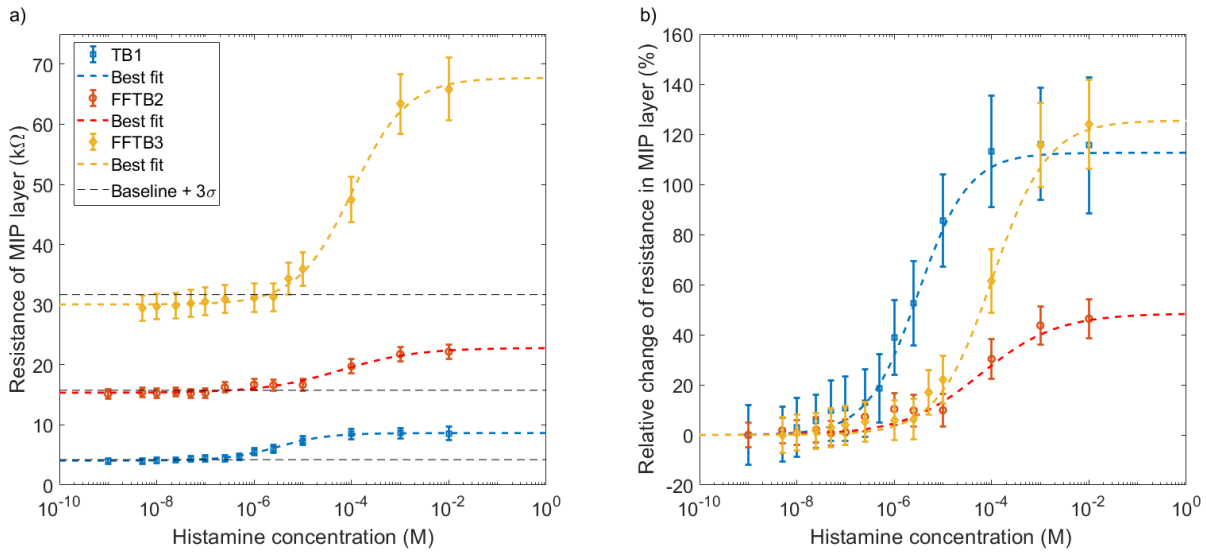

Figure 5. Dose response curves of the functionalized CIs by fitting the 5 element EEC to the impedance spectra, such as displayed in Figure 4. a) the ohmic resistance of the MIP sensor layer in function of histamine. Dashed line is the best sigmoid response function fit (Eq. 1). Error bars indicate 95% margin of error. b) Relative change of the ohmic resistance of the MIP sensor layer by dividing the values in the left figure by the resistance of the MIP layer in the absence of histamine.

Table 1. Best fitting result of the dose response function (Eq. 1) as displayed graphically in Figure 5.

	R(c=0)	A	ED_{50}	S	R^2	LOD
TB1	4.0 ± 0.1 kΩ	4.6 ± 0.1 kΩ	3.0 ± 0.1 µM	0.84 ± 0.06	0.997	200 nM
FFTB2	15.3 ± 0.25 kΩ	7.5 ± 0.8 kΩ	59 ± 6 µM	0.55 ± 0.13	0.978	1 µM
FFTB3	30.0 ± 0.5 kΩ	38.0 ± 1.5 kΩ	105 ± 17 µM	0.77 ± 0.07	0.997	5 µM

3.4. Changes in artificial perilymph conductivity and interfacial double layer capacitance

As the concentration of histamine changes in the artificial perilymph, so will the concentration of anions and cations which influence the electrical conductivity of the liquid. This change can be observed in parameter Rs of the 5-element model, which is a sum of the (static) cable resistance and the (changing) artificial perilymph resistance. Besides changing the conductivity of the liquid, a different histamine concentration will also affect the interfacial double layer capacity Cdl and the diffusion driven Warburg impedance Aw. A comparison of these three parameters Rs, Cdl and Aw in function of histamine concentration is given in Figure 6, alongside the MIP sensor layer capacitance C1 as found in the EEC. A dashed line is provided for each sample as a linear fit of the parameter in function of the base-10 logarithm of the histamine concentration, mainly as a visual aid. Error bars represent the 95% margin of error of the obtained fit parameter value. All series resistance values decrease for increasing histamine concentration. All double layer capacitance increasesd for increasing histamine concentration and with the exception of TB1, the Warburg impedance also increased for increasing concentration.

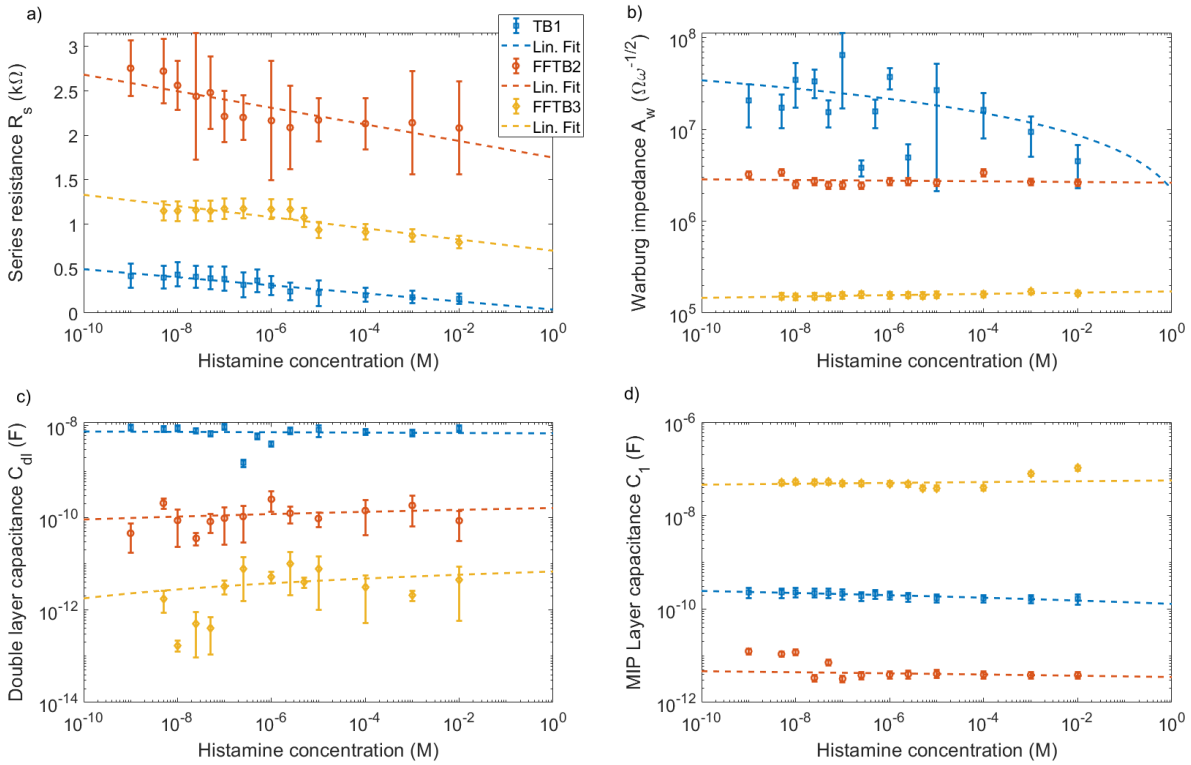

Figure 6. Remaining fitting parameters of the 5-element model in function of histamine concentration. a) Series resistance, a sum of the wire and the liquid resistance. b) Diffusion driven Warburg impedance c) Interfacial double layer capacitance and d) MIP sensor layer capacitance. Individual datapoints are the best fit values for the EEC model, dashed lines are a

linear fit as a visual aid to identify trends. Error bars indicate the 95% margin of error for the obtained fit parameter. Panel a) has the Y-axis on a linear scale, while b), c) and d) are on a log10 scale for the Y-axis due to the large spread of values over the 3 samples. Error bars are obtained on a linear scale and appear asymmetrical due to log10 Y axis.

3.5. Coating integrity

Before and after insertion of the functionalized CI into the cochlea, the coating was inspected with a microscope using a Z-axis focus stacking technique. The rough texture of the MIP coating, in combination with the curvature of the CI (640 µm diameter) and the poorly-conductive nature of the MIP coating prohibited the use of other inspection techniques such as Atomic Probe Microscopy or Scanning Electron Microscopy. Large protruding clusters of MIP particles were prone to breaking of during insertion or during the flushing cycles. A comparison is given in Figure 7; the coating on the electrodes remained intact, while the flexible silicone part of the implant showed missing MIP pieces. Once inside the cochlea, the average thickness of the coating can be monitored via the capacitance of the MIP coating (C1 in the 5-element model), displayed graphically in Figure 6, alongside a linear fit for visual aid. In all samples the MIP layer capacitance display small in- or decreasing trends but appear stable overall.

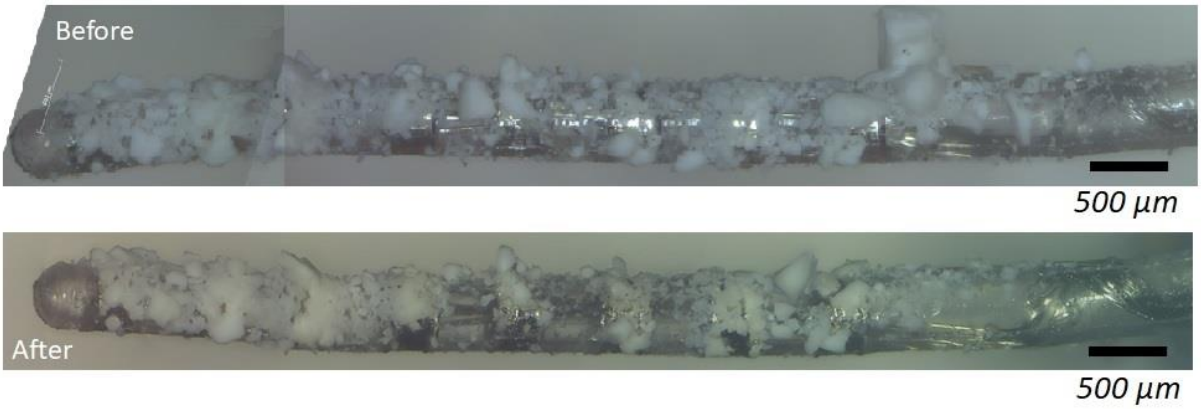

Figure 7. Stitched microscope photograph comparison of the MIP coating on a CI (Top) before and (Bottom) after insertion into the scala tympani of the cochlea. Large protruding clusters of MIP particles were prone to breaking off during insertion or during the flushing cycles. Scale bar is 500 µm.

4. Discussion

The use of artificial perilymph in lieu of native perilymph in the frequency range of 100 Hz to 100 kHz does not change the local impedimetric response as measured by the electrodes of a CI inside the scala tympani of a human cadaver cochlea. The presence of human serum albumin

instead of cells does create a larger capacitance and lower impedance at frequencies below 100 Hz, presumably due to surface absorption of the albumin onto either the electrode surface or the MIP sensor layer. Opposed to previously published EEC models on MIP bioreceptors, this does necessitate the introduction of a significant double layer capacitance at the sensor-liquid interface, resulting in a total of five fitting parameters. This element is necessary to obtain a meaningful fitting and to reach a correct value for the ohmic resistance of the MIP sensor coating, correlated to the concentration of the analyte.

The recorded impedance spectra differ in both impedance baselines and sensitivity to increasing histamine concentration. This is a direct consequence of the differences in coating thickness for the different CIs. Against intuition, the thinnest coating (FFTB2) resulted in the highest overall impedance. The thin coating allowed for a higher impedimetric combination of Warburg- and interfacial double layer impedance. The thickest coating (FFTB3) yielded the lowest Warburg- and interfacial double layer impedance, while having the highest MIP layer impedance. The ohmic resistance of the MIP layer scales with thickness and reduces the charge transfer between liquid and electrode responsible for the double layer capacitance and diffusion driven constant phase impedance. The thickest coating also has the highest level of detection at 5 µM and when fully saturated has increased by more than 100% in impedance. Physiological concentration of histamine is approximately 10 nM, while an acute inflammation can increase the concentration to the range of 10 µM to 100 µM. [42] meaning all sensors are capable of detecting this type of inflammation.

The implant inserted in TB1, with a total MIP coverage of the electrode without being excessive, has the best level of histamine detection at 200 nM. It does have the lowest MIP layer resistance and is characterized by the associated highest Warburg and double layer capacitance. Despite this, it also doubles in absolute impedance value upon saturation.

While the (biocompatible) PMMA-based coating on the platinum-iridium electrodes remains intact and functional after insertion, the poor adhesion to the silicone part of the implant and the rough, jagged surface of the bioreceptor layer does raise concern for continuation to in vivo or clinical studies. Pieces that detach may result in a foreign body reaction or impede cochlear functionality of, for example, low frequency residual hearing. The increase in electrode array diameter above 900 µm increases the risk of trauma by rubbing contact between CI and soft tissue in the cochlea. A trivial solution towards future improvements is to mechanically clean the non-electrode parts of the implant of MIP coating. While the surface roughness of the coating could damage inner ear soft tissue, a much thinner, smoother coating, such as the coating used in FFTB2 greatly reduces these risks, but at the cost of decreased sensitivity (LoD

of 1 µM vs 200 nM and only 40% increase in impedance vs. 115%) to the extent that it might fall short of the, yet unknown, physiological range.

Individual chemical sensors cannot be calibrated, the extraction process would damage the implant, as to provide the exact histamine concentration, but rather functions as an indicator for histamine concentration above 200 nM. In post-operative settings where the main function is to be an early warning system for inflammation were histamine levels are typically expressed in several or tens of micromolar, this functionality is sufficient.[43] For future fundamental research use where the exact concentration of histamine needs to be known, e.g., for objective measurements of anti-inflammatory pharmaceuticals, a standardized batch-style production can be employed where electrodes are sampled and indicative of the dose-response of the rest of the synthesized batch.

Part of the acute inflammation pathway was simulated by replenishing the cochlear fluid with a known concentration and assuming the contents of the scala tympani matches that of the injected spiked perilymph. It must be noted that very little is known on the leaking of the artificial perilymph towards other parts of the inner ear, such as to the vestibular organ (balance organ). This may play an important role during in-vivo measurements of histamine with a functionalized CI where histamine is released directly into the scala tympani and can diffuse, as opposed to this study, where an abundance of spiked perilymph was provided. The acute nature of these experiments means little information is available on long-time effects such as biofouling and foreign body reaction.

5. Conclusions

Analysis of the dose response of three PMMA-based histamine-sensitive MIPs of different thickness of CI electrode arrays indicates viability as an intracochlear receptor coating, useful for the detection of inflammation in the hearing organ after CI insertion surgery. These proof-of-concept results highlight both feasibility and points of improvement for clinical application, such as a coating that is smooth and with a clear option for calibration, good adhesion to the metal electrodes, while at the same time preventing adhesion to the implants silicone.

Supporting Information

Supporting Information is available from the Wiley Online Library or from the author.

Acknowledgements

TP acknowledges funding by the research foundation Flanders (FWO G088619N) and the KU Leuven internal grant (IDN/21/021). NV acknowledges funding by the research foundation Flanders (FWO 1804821N). GW acknowledges funding by the research foundation Flanders (FWO G.0B25.14.N). MW acknowledges funding by the research foundation Flanders (FWO G0B3218N). MP Acknowledges funding by the Engineering and Physical Sciences Research Council (EPSRC EP/W031590/1). Cochlear Ltd. and Hannover Medical School (MHH) kindly provided the CI electrodes used.

Received: ((will be filled in by the editorial staff))
Revised: ((will be filled in by the editorial staff))
Published online: ((will be filled in by the editorial staff))

References

[1] B. S. Wilson and M. F. Dorman, "Cochlear implants: A remarkable past and a brilliant future," *Hear. Res.*, vol. 242, no. 1–2, pp. 3–21, Aug. 2008, doi: 10.1016/J.HEARES.2008.06.005.

[2] A. A. Eshraghi, N. W. Yang, and T. J. Balkany, "Comparative study of cochlear damage with three perimodiolar electrode designs," *Laryngoscope*, vol. 113, no. 3, pp. 415–419, Mar. 2003, doi: 10.1097/00005537-200303000-00005.

[3] N. Schart-Morén, S. K. Agrawal, H. M. Ladak, H. Li, and H. Rask-Andersen, "Effects of Various Trajectories on Tissue Preservation in Cochlear Implant Surgery: A Micro-Computed Tomography and Synchrotron Radiation Phase-Contrast Imaging Study," *Ear Hear.*, vol. 40, no. 2, pp. 393–400, Mar. 2019, doi: 10.1097/AUD.0000000000000624.

[4] A. Starovoyt, T. Putzeys, J. Wouters, and N. Verhaert, "High-resolution Imaging of the Human Cochlea through the Round Window by means of Optical Coherence Tomography," *Sci. Rep.*, vol. 9, no. 1, pp. 1–10, Dec. 2019, doi: 10.1038/s41598-019-50727-7.

[5] A. Starovoyt *et al.*, "An optically-guided cochlear implant sheath for real-time monitoring of electrode insertion into the human cochlea," *Sci. Reports 2022 121*, vol. 12, no. 1, pp. 1–12, Nov. 2022, doi: 10.1038/S41598-022-23653-4.

[6] A. Soda-Merhy, L. Gonzalez-Valenzuela, and C. Tirado-Gutierrez, "Residual hearing preservation after cochlear implantation: Comparison between straight and perimodiolar implants," *Otolaryngol. - Head Neck Surg.*, vol. 139, no. 3, 2008, doi:

10.1016/j.otohns.2008.06.006.

[7] A. Al Omari, A. Nuseir, M. B. Ata, L. Khasawneh, A. Alhowary, and F. Alzoubi, "Accuracy of intraoperative electrophysiological testing in confirming correct cochlear implant electrode positions," *Cochlear Implants Int.*, vol. 20, no. 6, pp. 324–330, Nov. 2019, doi: 10.1080/14670100.2019.1656904.

[8] V. Scheper *et al.*, "Local inner ear application of dexamethasone in cochlear implant models is safe for auditory neurons and increases the neuroprotective effect of chronic electrical stimulation," *PLoS One*, vol. 12, no. 8, Aug. 2017, doi: 10.1371/journal.pone.0183820.

[9] J. Zhang, W. Wei, J. Ding, T. Roland, S. Manolidis, and N. Simaan, "Inroads toward robot-assisted cochlear implant surgery using steerable electrode arrays," in *Otology and Neurotology*, Oct. 2010, vol. 31, no. 8, pp. 1199–1206, doi: 10.1097/MAO.0b013e3181e7117e.

[10] G. M. Kalinec, G. Lomberk, R. A. Urrutia, and F. Kalinec, "Resolution of Cochlear Inflammation: Novel Target for Preventing or Ameliorating Drug-, Noise- and Age-related Hearing Loss," *Front. Cell. Neurosci.*, vol. 11, Jul. 2017, doi: 10.3389/FNCEL.2017.00192.

[11] D. Gilroy and R. De Maeyer, "New insights into the resolution of inflammation," *Seminars in Immunology*, vol. 27, no. 3. Semin Immunol, pp. 161–168, May 01, 2015, doi: 10.1016/j.smim.2015.05.003.

[12] S. E. Headland and L. V. Norling, "The resolution of inflammation: Principles and challenges," *Seminars in Immunology*, vol. 27, no. 3. Semin Immunol, pp. 149–160, May 01, 2015, doi: 10.1016/j.smim.2015.03.014.

[13] J. P. Harris, "Immunology of the inner ear: Response of the inner ear to antigen challenge," *Otolaryngol. Neck Surg.*, vol. 91, no. 1, pp. 18–23, 1983, doi: 10.1177/019459988309100105.

[14] M. D. Frye, W. Yang, C. Zhang, B. Xiong, and B. H. Hu, "Dynamic activation of basilar membrane macrophages in response to chronic sensory cell degeneration in aging mouse cochleae," *Hear. Res.*, vol. 344, pp. 125–134, 2017, doi: 10.1016/j.heares.2016.11.003.

[15] W. Zhang *et al.*, "Perivascular-resident macrophage-like melanocytes in the inner ear are essential for the integrity of the intrastrial fluid-blood barrier," *Proc. Natl. Acad. Sci. U. S. A.*, vol. 109, no. 26, pp. 10388–10393, Jun. 2012, doi: 10.1073/pnas.1205210109.

[16] Y. Zhang *et al.*, "The Detrimental and Beneficial Functions of Macrophages After Cochlear Injury," *Front. Cell Dev. Biol.*, vol. 9, p. 631904, Aug. 2021, doi: 10.3389/FCELL.2021.631904.

[17] A. D. Claussen *et al.*, "Chronic cochlear implantation with and without electric stimulation in a mouse model induces robust cochlear influx of CX3CR1+/GFP macrophages," *Hear. Res.*, vol. 426, Dec. 2022, doi: 10.1016/J.HEARES.2022.108510.

[18] T. Kaur, D. Mukherjea, K. Sheehan, S. Jajoo, L. P. Rybak, and V. Ramkumar, "Short interfering RNA against STAT1 attenuates cisplatin-induced ototoxicity in the rat by suppressing inflammation," *Cell Death Dis.*, vol. 2, no. 7, Jul. 2011, doi: 10.1038/cddis.2011.63.

[19] M. Fujioka, S. Kanzaki, H. J. Okano, M. Masuda, K. Ogawa, and H. Okano, "Proinflammatory cytokines expression in noise-induced damaged cochlea," *J. Neurosci. Res.*, vol. 83, no. 4, pp. 575–583, Mar. 2006, doi: 10.1002/jnr.20764.

[20] T. Okano *et al.*, "Bone marrow-derived cells expressing Iba1 are constitutively present as resident tissue macrophages in the mouse cochlea," *J. Neurosci. Res.*, vol. 86, no. 8, pp. 1758–1767, 2008, doi: 10.1002/jnr.21625.

[21] H. L. Haas, O. A. Sergeeva, and O. Selbach, "Histamine in the nervous system," *Physiological Reviews*, vol. 88, no. 3. American Physiological Society, pp. 1183–1241, Jul. 2008, doi: 10.1152/physrev.00043.2007.

[22] F. Borriello, R. Iannone, and G. Marone, "Histamine release from mast cells and basophils," in *Handbook of Experimental Pharmacology*, vol. 241, Springer Science and Business Media, LLC, 2017, pp. 121–139.

[23] D. Laroche, P. Gomis, E. Gallimidi, J. M. Malinovsky, and P. M. Mertes, "Diagnostic value of histamine and tryptase concentrations in severe anaphylaxis with shock or cardiac arrest during anesthesia," *Anesthesiology*, vol. 121, no. 2, pp. 272–279, Aug. 2014, doi: 10.1097/ALN.0000000000000276.

[24] D. Morgan, I. Moodley, M. J. Phillips, and R. J. Davies, "Plasma histamine in asthmatic and control subjects following exercise: influence of circulating basophils and different assay techniques," *Thorax*, vol. 38, pp. 771–777, 1983, doi: 10.1136/thx.38.10.771.

[25] A. Di Lorenzo, C. Fernández-Hernando, G. Cirino, and W. C. Sessa, "Akt1 is critical for acute inflammation and histamine-mediated vascular leakage," *Proc. Natl. Acad. Sci.*, vol. 106, no. 34, pp. 14552–14557, Aug. 2009, doi: 10.1073/PNAS.0904073106.

[26] H. Azuma, S. Sawada, S. Takeuchi, K. Higashiyama, A. Kakigi, and T. Takeda,

"Expression of mRNA encoding the H1, H2, and H3 histamine receptors in the rat cochlea," *Neuroreport*, vol. 14, no. 3, pp. 423–425, Mar. 2003, doi: 10.1097/00001756-200303030-00025.

[27] P. Panula, U. Pirvola, S. Auvinen, and M. S. Airaksinen, "Histamine-immunoreactive nerve fibers in the rat brain," *Neuroscience*, vol. 28, no. 3, pp. 585–610, 1989, doi: 10.1016/0306-4522(89)90007-9.

[28] S. Rubenwolf, S. Kerzenmacher, R. Zengerle, and F. Von Stetten, "Strategies to extend the lifetime of bioelectrochemical enzyme electrodes for biosensing and biofuel cell applications," *Applied Microbiology and Biotechnology*, vol. 89, no. 5. Appl Microbiol Biotechnol, pp. 1315–1322, Mar. 2011, doi: 10.1007/s00253-010-3073-6.

[29] G. Wackers *et al.*, "Towards a catheter-based impedimetric sensor for the assessment of intestinal histamine levels in IBS patients," *Biosens. Bioelectron.*, vol. 158, p. 112152, Jun. 2020, doi: 10.1016/j.bios.2020.112152.

[30] J. J. BelBruno, "Molecularly Imprinted Polymers," *Chem. Rev.*, vol. 119, no. 1, pp. 94–119, Jan. 2018, doi: 10.1021/ACS.CHEMREV.8B00171.

[31] E. C. Kirk and A. D. Gosselin-Ildari, "Cochlear labyrinth volume and hearing abilities in primates," *Anat. Rec.*, vol. 292, no. 6, pp. 765–776, Jun. 2009, doi: 10.1002/ar.20907.

[32] M. Khorshid, S. B. Sichani, P. Cornelis, G. Wackers, and P. Wagner, "The hot-wire concept: Towards a one-element thermal biosensor platform," *Biosens. Bioelectron.*, vol. 179, p. 113043, May 2021, doi: 10.1016/j.bios.2021.113043.

[33] M. Peeters *et al.*, "Impedimetric detection of histamine in bowel fluids using synthetic receptors with pH-optimized binding characteristics," *Anal. Chem.*, vol. 85, no. 3, pp. 1475–1483, Feb. 2013, doi: 10.1021/ac3026288.

[34] A. Starovoyt *et al.*, "Anatomically and mechanically accurate scala tympani model for electrode insertion studies," *Hear. Res.*, vol. 430, p. 108707, Mar. 2023, doi: 10.1016/J.HEARES.2023.108707.

[35] S. C. Bae, Y. R. Shin, and Y. M. Chun, "Cochlear Implant Surgery Through Round Window Approach Is Always Possible," *Ann. Otol. Rhinol. Laryngol.*, vol. 128, no. 6_suppl, pp. 38S-44S, Jun. 2019, doi: 10.1177/0003489419834311.

[36] T. Putzeys, A. Starovoyt, N. Verhaert, and M. Wübbenhorst, "The Dielectric Behavior of Human ex vivo Cochlear Perilymph," *IEEE Trans. Dielectr. Electr. Insul.*, vol. 28, no. 3, pp. 932–937, Jun. 2021, doi: 10.1109/tdei.2021.009515.

[37] J. C. Palmer *et al.*, "Development and performance of a biomimetic artificial perilymph

for in vitro testing of medical devices," *J. Neural Eng.*, vol. 16, no. 2, 2019, doi: 10.1088/1741-2552/aaf482.

[38] A. L. Hodgkin and A. F. Huxley, "A quantitative description of membrane current and its application to conduction and excitation in nerve," *J. Physiol.*, vol. 117, no. 4, pp. 500–544, Aug. 1952, doi: 10.1113/JPHYSIOL.1952.SP004764.

[39] Y. Wang and E. S. Olson, "Cochlear perfusion with a viscous fluid," *Hear. Res.*, vol. 337, pp. 1–11, Jul. 2016, doi: 10.1016/j.heares.2016.05.007.

[40] P. Pelliccia *et al.*, "Variabilità delle dimensioni cocleari e sue implicazioni nella pratica clinica," *Acta Otorhinolaryngol. Ital.*, vol. 34, no. 1, pp. 42–49, 2014, Accessed: Apr. 07, 2021. [Online]. Available: /pmc/articles/PMC3970226/.

[41] W. Stilman *et al.*, "Detection of yeast strains by combining surface-imprinted polymers with impedance-based readout," *Sensors Actuators B Chem.*, vol. 340, p. 129917, Aug. 2021, doi: 10.1016/J.SNB.2021.129917.

[42] F. András and K. Merétey, "Histamine: an early messenger in inflammatory and immune reactions," *Immunol. Today*, vol. 13, no. 5, pp. 154–156, 1992, doi: 10.1016/0167-5699(92)90117-P.

[43] S. Smolinska, M. Jutel, R. Crameri, and L. O'Mahony, "Histamine and gut mucosal immune regulation," *Allergy*, vol. 69, no. 3, pp. 273–281, Mar. 2014, doi: 10.1111/ALL.12330.

Supporting Information

Micro-CT image of Cochlear Implant electrode array in human cadaver cochlea, in temporal bone

Insertion of the CI electrodes in the scala tympani was verified with the aid of a microscope, but the exact position of the electrodes relative to the scala walls could only be verified with a µCT scan after the impedance measurements. To reduce dislocation during transport the external parts of the CI were tacked in place using Play-Doh (Hasbro). The advantage of using a small, rodent-size, CI is the low distortion of the image due to few platinum-iridium electrodes with high absorption of X-rays. Figure S1.1 is a cross section of a CT scan of a human cochlea containing a small, rodent-size, CI electrode array, with artifacts surrounding the metal contacts. The CI is completely inserted in the scala tympani and the 8 individual electrodes can be identified. In this case, only the electrodes at the tip of the array are not in close contact with soft tissue and will provide a representative perilymph measurement. The other electrodes will see a contribution of either modiolar wall, lateral wall, or basilar membrane in their impedance spectrum. Results from these electrodes will be omitted for histamine sensing.

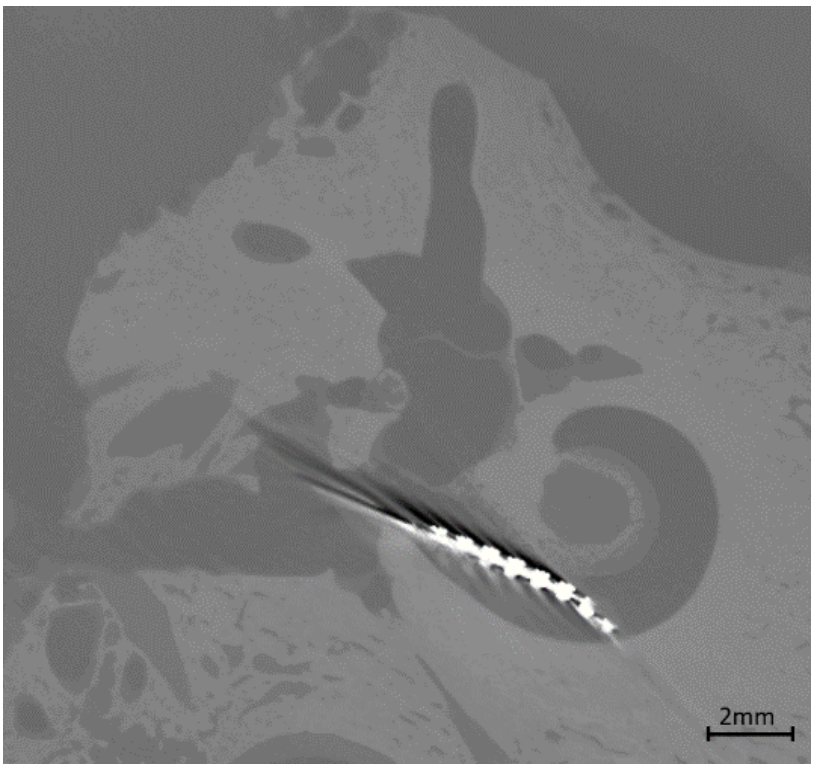

Figure S1: µCT cross section of human cochlea containing small, rodent size, CI electrode array. The metal electrodes introduce artifacts in the CT scan in the form of alternating bright and dark spots. Scale bar is 2mm.

Impedance spectra of histamine-spiked artificial perilymph as measured by CI electrodes in a human cadaver cochlea.

Variance in both PolyStyrene (PS) and MIP powder coating thickness result in variation in both initial impedance and change in impedance between samples. Increasing the concentration of histamine increases the overall impedance, though a different response above and below 3000 Hz is observed. In TB 1, there are periodic increases in high frequency impedance, possibly due to small fragments of soft tissue being introduced and removed via the periodic flushing through the stapes opening. In FFTB 2 the impedance first decreases slightly at +3000 Hz before increasing at higher histamine concentration. In FFTB 3 there is a significant increase at both low and high frequency impedance.

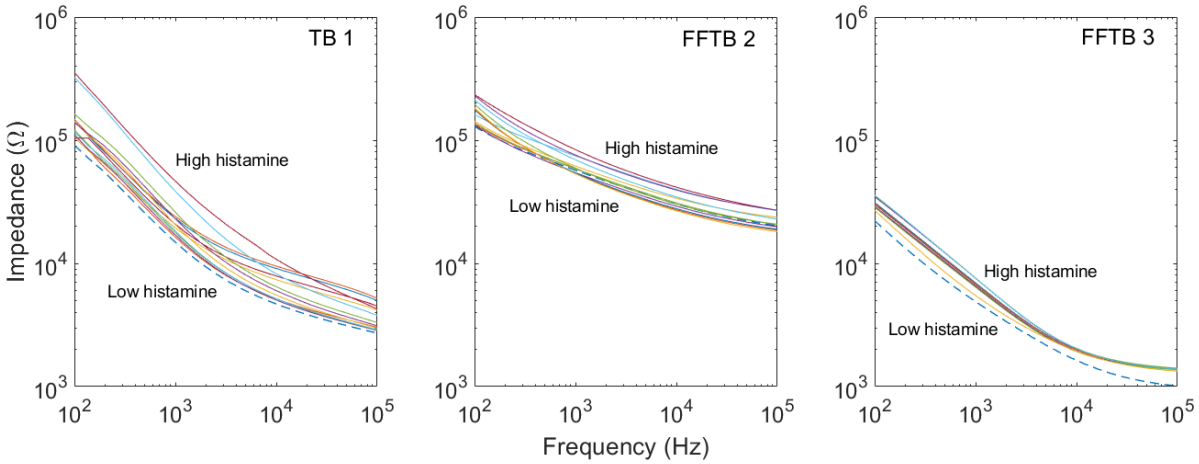

Figure S2: Impedance spectra of artificial perilymph as measured by a CI inside the scala tympani of a human cochlea for three temporal bones, one fresh (TB1) and two fresh frozen (FFTB 2 and FFTB 3). The lower, blue, dashed line represents the impedance of artificial perilymph without histamine. As histamine concentration increases from 1 nM to 10 mM, the general trend of the impedance curve is to increase. Even though coating conditions vary, there is a consistent trend that selective binding of histamine systematically increases the absolute impedance.